High-Temperature Oxidation of Aniline to Highly Ordered Polyaniline–Sulfate Salt with a Nanofiber Morphology and Its Use as Electrode Materials in Symmetric Supercapacitors

Srinivasan Palaniappan,[1] Singu Bal Sydulu,[2] Taneeru Lakshmi Prasanna,[1] Pabba Srinivas[2]

[1]*Organic Coatings and Polymers Division, Indian Institute of Chemical Technology, Hyderabad 500 607, India*
[2]*Department of Chemistry, Osmania University, Hyderabad 500 007, India*

Received 11 March 2010; accepted 21 July 2010
DOI 10.1002/app.33091
Published online 3 November 2010 in Wiley Online Library (wileyonlinelibrary.com).

ABSTRACT: In this study, for the first time, aniline was oxidized by ammonium persulfate (APS) at higher temperatures without any protic acid, and APS acted as an oxidizing agent and a protonating agent. During the oxidation of aniline by APS, sulfuric acid formation occurred, and the sulfuric acid was incorporated into polyaniline (PANI) as a dopant. PANI–sulfate samples were characterized by IR spectroscopy, X-ray diffraction, and scanning electron microscopy techniques. In this methodology, a highly ordered PANI–sulfate salt (H_2SO_4) with a nanofiber morphology was synthesized. Interestingly, a PANI base was also obtained with a highly ordered structure with an agglomerated netlike nanofiber morphology. PANI–H_2SO_4 was used as an electrode material in a symmetric supercapacitor cell. Electrochemical characterization, including cyclic voltammetry (CV), charge–discharge (CD), and impedance analysis, was carried out on the supercapacitor cells. In this study, the maximum specific capacitance obtained was found to be 273 F/g at 1 mV/s. Scan rate from cyclic voltammetry and 103 F/g at 1 mA discharge current from CD measurement. Impedance measurement was carried out at 0.6 V, and it showed a specific capacitance of 73.2 F/g. The value of the specific capacitance and energy and power densities for the PANI–H_2SO_4 system were calculated from CD studies at a 5-mA discharge rate and were found to be 43 F/g, 9.3 W h/kg, and 500 W/kg, respectively, with 98–100% coulombic efficiency. © 2010 Wiley Periodicals, Inc. J Appl Polym Sci 120: 780–788, 2011

Key words: conducting polymers; electrochemistry; electron microscopy; nanofiber; X-ray

INTRODUCTION

Supercapacitors, ultracapacitors, or electrochemical double-layer capacitors are commonly used names for a class of electrochemical energy-storage devices that are ideally suited to the rapid storage and release of energy during short pulses of time. Supercapacitors lie between conventional capacitors and batteries in design and performance.

When a metal (or an electronic conductor) is brought in contact with a solid or liquid ionic conductor, a charge accumulation is achieved electrostatically on either side of the interface; this leads to the development of an electrical double-layer, which is essentially a molecular dielectric. No charge transfer takes place across the interface, and the current observed during this process is essentially a displacement current due to the rearrangement of charges (conventionally described as an ideally polarized electrode). Therefore, this process is nonfaradaic in nature. Also, the charge storage is achieved by an electron transfer that produces oxidation state changes in the electrostatic materials according to Faraday's laws in relation to electrode potentials (the so-called ideally reversible electrode). Thus, this process is faradaic in nature. Accordingly, two types of supercapacitors have been studied.[1,2] One operates by charging and discharging the interfacial electrical double layer. In the second type, often called a pseudocapacitor or redox capacitor, the charge–discharge mechanism involves the transfer of an electrical charge between the phases but without any bulk-phase transformation. The electrons involved in the nonfaradaic electrical double-layer charging are the itinerant conduction-band electrons of the metal or carbon electrode, whereas the electrons involved in the faradaic processes are transferred to or from valence-electron states (orbitals) of the redox cathode or anode reagent. The electrons may, however, arrive in or depart from the conduction-band states of the electronically conducting support material, depending on whether the Fermi level in the electronically conducting support lies below

Correspondence to: S. Palaniappan (palaniappan@iict.res.in, palani74@rediffmail.com).

the highest occupied state of the reductant or above the lowest unoccupied state of the oxidant. In pseudocapacitors, the nonfaradaic double-layer charging process is usually accompanied by a faradaic charge transfer.[3]

Four main classes of materials are described for supercapacitors in the literature: metal oxides, electronically conducting polymers, carbons, and hybrid materials. Many reviews on supercapacitors have been reported in the literature, and recent reviews are given here for reference.[1,2,4–6] In particular, conducting polymers represent an attractive class of materials for use as electrodes in electrochemical capacitors because of their advantageous properties, which include fast doping–dedoping during charge–discharge, high charge density, easy synthesis, and low cost compared to noble metal oxides. Among the various conducting polymers, polyaniline (PANI) holds great promise because of its multiple electronic states, high conductivity that occurs with doping, and easy and economic preparation and good environmental stability. PANI falls under the category of pseudo supercapacitors or redox capacitors, wherein the capacitance comes from faradaic reactions at the electrode–electrolyte surface. PANIs are attractive for use as electrochemical capacitors because of their combination of a high charge density, rapid reduction, and oxidation reaction in the whole bulk phase compared with carbon materials and low cost compared with metal oxides. The literature status of supercapacitors based on chemically synthesized PANI[7–26] during the years 2007–2010 is given in Table I.

PANI synthesized by chemical or electrochemical methods has been investigated through the performance of electrode materials in supercapacitors. PANI synthesized by chemical method has advantages compared to that synthesized by electrochemical methods. In the electrochemical method, the mass production of composite electrodes is not possible, and also, this method not suitable for preparing controlled polymer films with thicknesses above 100 μm.

In this study, for the first time, a PANI–sulfate salt (H_2SO_4) was synthesized by the oxidation of aniline at higher temperatures with ammonium persulfate (APS) without any protic acid. We synthesized PANI–H_2SO_4 salts by changing the concentration of oxidant, the reaction time, and the temperature. PANI–H_2SO_4 salts were characterized with Fourier transform infrared (FTIR) spectroscopy, X-ray diffraction (XRD), and scanning electron microscopy (SEM). The performance of the PANI–H_2SO_4 salts as electrode materials for supercapacitors were investigated with cyclic voltammetry (CV), galvanostatic charge–discharge (CD), and electrochemical impedance spectral (EIS) analyses.

TABLE I
Literature Reports on PANI Supercapacitors During the Years 2007–2010

System	Electrolyte	Capacitance (F/g)	Reference
AC–AC–H_2SO_4 (AC prepared from PANI)	6*M* KOH	235	7
PANI–MC	10 wt % H_2SO_4	96	8
PANI–OMC	30 wt % KOH	747	9
PANI nanorods	0.1*M* H_2SO_4	592	10
PANI nanospheres		294	
PANI–graphene oxide	1*M* H_2SO_4	531	11
PANI–Zn	NH_4Cl–$ZnCl_2$	400	12
PANI–SnO_2	1*M* H_2SO_4	305	13
PANI–TiO_2	1*M* H_2SO_4	330	14
PANI	1*M* H_2SO_4	428	15
PANI–PPy	1*M* H_2SO_4	416	16
PANI–MWCNTs	1*M* H_2SO_4	554	17
PANI–NAFION–RuO_2	1*M* H_2SO_4	475	18
PANI–MWCNTs	$NaNO_3$	328	19
PANI–MWNTs	1*M* H_2SO_4	322	20
GNS–CNT–PANI	6*M* KOH	1035	21
GNS–PANI		1046	
PANI		115	
CCDC–PANI	1*M* H_2SO_4	713.4	22
PANI–nanofibers	1*M* H_2SO_4	298	23
PANI–CNT	1*M* $NaNO_3$	20	24
PANI–HBF_4	1*M* H_2SO_4	140	25
PANI–graphite	1*M* H_2SO_4	–	26

AC = activated carbon; MC = mesoporous carbon; OMC = ordered mesoporous carbon; MWCNTs = multiwalled carbon nanotubes; GNS = graphene nanosheet; CNT = carbon nanotubes; CCDC = calcium carbide derived carbon; PPy = polypyrrole.

EXPERIMENTAL

Materials

Aniline (S. D. Fine Chemicals, Mumbai, India) was purified under reduced pressure. APS, sodium hydroxide, and sulfuric acid (Rankem, India) were used as received. All of the reactions were carried out with distilled water. Solvents were distilled and used.

Synthesis of the PANI salts

PANI was synthesized by the chemical oxidative polymerization of aniline. In a typical experiment, 1 mL of aniline (0.2*M*) was dissolved in 25 mL of distilled water in a 100-mL round-bottom flask and kept in an oil bath at 60°C with constant stirring. APS (2.51 g, 0.2*M*) was dissolved in 30 mL of water and added dropwise to the previous solution for around 18–20 min under constant stirring. The resulting reaction mixture was stirred for 6 h at 60°C. The precipitate was filtered and washed with an ample amount of water and, finally, with 250 mL

TABLE II
Yield, Conductivity, Number of Dopant Units per 4 Aniline Units, and Specific Capacitance of PANI Salt Prepared Under Different Conditions

Variation	Formula-based yield (%)	Conductivity (S/cm)	Dopant units[a]	Specific capacitance (F/g) From CV[b] 1	From CV[b] 5	From CV[b] 10	From CD[c] 1	From CD[c] 5
APS (M)[d]								
0.20	66	1.2×10^{-6}	0.9	11	4	2	1	–
0.25	64	8.7×10^{-6}	1.3	106	58	27	45	2
0.30	77	6.8×10^{-4}	1.3	182	73	35	70	40
0.35	81	1.7×10^{-4}	1.1	100	44	20	61	26
0.40	81	8.1×10^{-6}	1.2	12	4	2	6	2
Time (h)[e]								
1	78	3.1×10^{-4}	1.4	138	79	49	86	44
2	77	3.1×10^{-4}	1.3	248	136	77	84	40
3	84	3.7×10^{-5}	1.3	273	154	96	103	43
4	82	5.9×10^{-4}	1.4	140	67	31	–	–
6	76	1.6×10^{-4}	1.3	182	73	35	70	40
Temperature (°C)[f]								
RT	64	1.3×10^{-3}	1.9	152	117	74	94	34
50	78	5.9×10^{-5}	1.4	160	84	84	104	48
60	77	1.6×10^{-4}	1.3	182	73	35	70	40
70	76	7.8×10^{-5}	1.2	128	57	27	49	7
80	84	7.1×10^{-5}	0.9	153	111	76	75	21
90	81	2.4×10^{-4}	0.9	166	127	87	56	1
100	79	1.0×10^{-8}	0.8	8	3	2	45	6

[a] Number of dopant units per 4 units of aniline in the PANI chain.
[b] CV scanned at 1, 5, and 10 mV/s.
[c] CD carried out at current densities of 1 and 5 mA.
[d] Reaction conditions: 1.0 mL of aniline, time = 6 h, temperature = 60°C, and various concentrations of APS (*M*).
[e] Reaction conditions: 1.0 mL of aniline, 0.3*M* APS, temperature = 60°C, and various time intervals.
[f] Reaction conditions: 1.0 mL of aniline, time = 6 h, 0.3*M* APS, and various temperature conditions.

of acetone. The powder sample was dried at 50°C to a constant weight. We also prepared PANI salts by changing the concentration of APS, the reaction time, and the temperature. The results are reported in Table II.

Synthesis of the PANI base

We dedoped PANI salts prepared by our method to PANI bases by stirring 0.5 g of PANI salt in 50 mL of a 1*M* aqueous sodium hydroxide solution for 12 h at ambient temperature. The solution was filtered and washed with 50 mL of a 1*M* aqueous sodium hydroxide solution, 250 mL of distilled water, and finally, 50 mL of acetone. The powder sample was dried at 50°C to a constant weight, and this weight was taken to be the weight of the PANI base.

Instrumentation and procedure

PANI–H_2SO_4 samples were pressed into disks 13 mm in diameter and about 1.5 mm in thickness under a pressure of 120 kg/cm^2. The resistance of samples was measured by two-probe method with a digital multimeter (model 2010, Keithely, Cleveland, OH). The resistance was calculated on the basis of the average value of three different pellets. The polymer samples for FTIR analysis were mixed with KBr powder and compressed into pellets, wherein the sample powder was evenly dispersed. FTIR spectra were recorded with a GC-FTIR spectrometer (model 670, Nicolet Nexus, Minnesota). XRD profiles for the PANI–H_2SO_4 powders were obtained on a Bruker AXS D8 advance X-ray diffractometer (Karlsruche, Germany) with Cu Kα radiation (land continuous) at a scan speed of 0.045°/min. Morphology studies of the polymer samples were carried out with a Hitachi S-3400N scanning electron microscope (Hitachi, Tokyo, Japan) operating at 20 kV. The sample was mounted on a carbon disc with the help of double-sided adhesive tape and sputter-coated with a thin layer of gold to prevent sample charging problems. CV and galvanostatic CD experiments were carried out with a WonATech multichannel potentiostat–galvanostat (WMPG1000, GyeongGi-do, Korea). Electrochemical impedance spectra were recorded with an IM6ex instrument (Zahner-Elektrik, 96317 Kronach, Germany). We prepared the PANI–H_2SO_4 electrode

material by mixing 80% polymer material with 20% battery-grade carbon and then pressing the mixture on stainless steel mesh (size = 24 μm) by the application of 100 kg/cm^2 of pressure. Three electrode cell measurements were carried out with PANI–H_2SO_4 as a working electrode, a platinum electrode as a counter electrode, and Ag/AgCl as a reference electrode in 1*M* H_2SO_4 electrolyte. The capacitor cell was constructed with two copolymer electrodes in 1*M* H_2SO_4 electrolyte.

Dopant unit, yield, and conductivity of the PANI salt

The amount of dopant (sulfuric acid) present on the PANI salt was calculated from the weight of the PANI salt used and the PANI base obtained in the dedoping process. The number of sulfuric acid dopant groups (n) present on the PANI salt was calculated from the amount of dopant present on the PANI salt, and the results are included in Table II:

$$\text{Dopant (\%)} = \frac{\text{Weight of polyaniline salt} - \text{Weight of polyaniline base}}{\text{Weight of polyaniline salt}} \times 100$$

$$n = \frac{\text{Dopant (\%)} \times \text{Molecular weight of aniline}}{(100 - \text{Weight loss}) \times \text{Molecular weight of } H_2SO_4}$$

The number of dopant units present on the PANI salt prepared at room temperature (RT) was found to be 1.9, which was close to the reported value (2.0). PANI salts prepared at higher temperatures showed lower numbers of dopant units on the PANI salt (0.8–1.4). One of the reasons for this low value of dopant units may have been the incomplete removal of dopant in the dedoping process.

The yield of PANI–H_2SO_4 was calculated on the basis of the PANI formula and included the dopant units, and the results are included in Table II. The yield of PANI–H_2SO_4 was found to be 76–84% with a reaction time of 1–6 h. The yield of PANI–H_2SO_4 increased with increasing concentration of APS. The yield of PANI–H_2SO_4 prepared at high temperatures (78–84%) was found to be higher compared to that of the RT reaction (64%). The observation of higher yield was due to the increase in the rate of the reaction.

The conductivity value of PANI–H_2SO_4 increased with increasing concentration of APS and then decreased with further increasing concentration. The conductivity of PANI–H_2SO_4 was nearly the same with the reaction time (Table II). The conductivity of PANI–H_2SO_4 prepared at RT (1.3×10^{-3} S/cm) was found higher than that of the PANI–H_2SO_4 prepared at high temperature. The conductivity of the PANI salts was found to be nearly the same (5.9×10^{-5} to 1.6×10^{-4} S/cm) with the reaction temperature (50–90°C). However, the conductivity was decreased drastically to 1×10^{-8} S/cm at 100°C. The effect of the decrease in conductivity with increasing temperature may have been due to overoxidation process or the fact that the kinetic effects were favored in the oxidation of aniline. This was in good agreement with a previous report in the literature.[27]

The previously discussed results show that in the case of the high-temperature oxidation of aniline to PANI salt, a reasonably good yield (77%) with a conductivity of 1.6×10^{-4} S/cm of PANI salt (Table II) was obtained with the use of aniline (0.1*M*) and APS (0.3*M*) at a temperature of 60°C and a time of 6 h.

RESULTS AND DISCUSSION

The structure of PANI is known to be a paralinked phenyleneamineimine. The emeraldine base (EB) form of PANI can, in principle, be described by the general formula shown in Figure 1(a). In the generalized base form, y measures the reduced units and $1 - y$ measures the fraction of oxidized units.[28,29] When $1 - y = 0$, the polymer has no such oxidized groups and is commonly known as a *leucoemeraldine base.* The fully oxidized form, $1 - y = 1$, is referred to as a *pernigraniline base.* The half-oxidized polymer, where the number of reduced units and oxidized units are equal, that is, $1 - y = 0.5$, is of special importance and is termed as the *emeraldine oxidation state* or EB. EB is electrically not conducting because of an empty conduction band, but doping with a strong acid both protonates iminic nitrogen and forms emeraldine salt [ES; Fig. 1(b)], which is electrically conducting by virtue of its half-filled polaron band.

In this study, aniline was oxidized by APS to PANI–H_2SO_4 at ambient temperature without any protic acid (Scheme 1), wherein APS was converted to sulfuric acid during the oxidation of aniline and doped on PANI system as a dopant.

S1

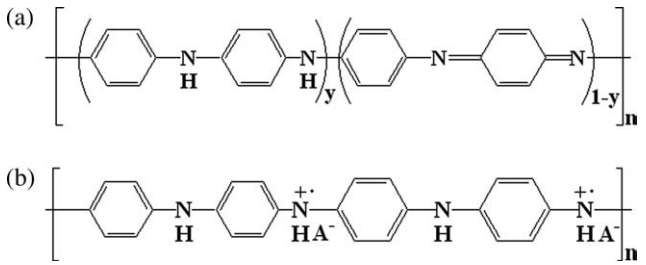

Figure 1 General structure of PANI in (a) EB and (b) ES forms.

FTIR spectra

The IR spectra of the PANI salt prepared at 60°C and its corresponding base are shown in Figure 2. The PANI base showed its characteristic bands [Fig. 2(a)] at 3450 cm^{-1} (N—H stretching); 3055 (w), 2965 (s), 2925, and 2850 cm^{-1} (—C—H stretching); 1560 cm^{-1} (C=C stretching of the quinonoid ring); 1500 cm^{-1} (C=C stretching of the benzenoid ring); 1375 and 1300 cm^{-1} (–C—N stretching]); 1145 cm^{-1} (electronic band or a vibrational band of the nitrogen quinine); 820 cm^{-1} (C—H out-of-plane bending for a 1,4-substituted benzene); and 695 cm^{-1} (aromatic ring deformation); these bands were similar to those of the standard PANI base.[30,31] In addition, the PANI base showed a small peak at 1045 cm^{-1}, which indicated the presence of a sulfate group. The IR spectrum of PANI–H_2SO_4 [Fig. 2(b)] showed all of the previous peaks for the PANI base, and in addition, it showed two more peaks, one at 3235 cm^{-1} (due to N—H^+), which designated that the formation of the PANI salt, and another intense peak at 1045 cm^{-1} (due to O=S=O[32]), which suggested the presence of H_2SO_4 on the PANI salt. These results supported the formation of the PANI salt containing H_2SO_4 dopant. All of the IR spectral behavior of the PANI–H_2SO_4's and their corresponding bases prepared at various experimental conditions in this study showed behavior similar that reported previously.

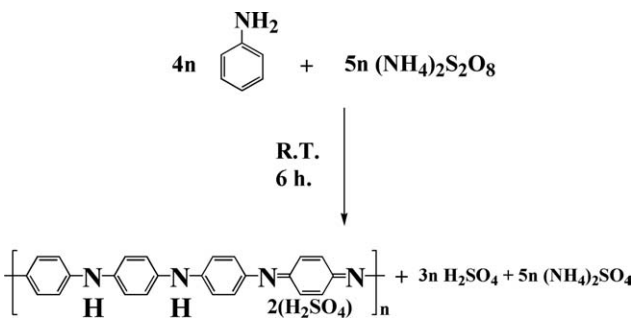

Scheme 1 Synthesis of PANI–H_2SO_4.

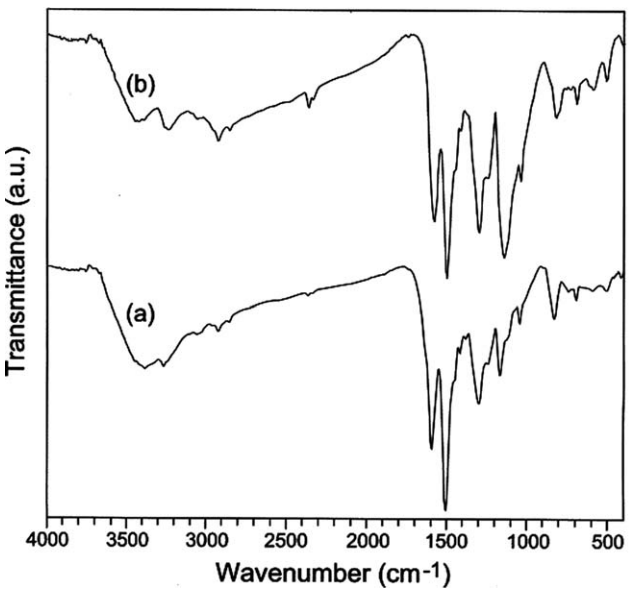

Figure 2 IR spectra of PANI (a) base and (b) salt.

XRD studies

The XRD spectra of all of the PANI–H_2SO_4 salts prepared in this study showed a similar pattern. As a representative system, PANI–H_2SO_4 salt prepared at 60°C showed intense peaks at 2θ = 6.4, 18.8, 19.8, 23.5, 25.8, and 28.2°, which corresponded to *d*-spacings of 13.7, 4.7, 4.5, 3.8, 3.4, and 3.2, respectively [Fig. 3(b)]. Peaks at 2θ = 23.5, 25.8, and 28.2° are characteristic of the ES of PANI.[33] The peaks at 19.8 and 18.5° were assigned to the periodicity parallel and perpendicular to the polymer chain, respectively. A remarkably narrow and intensive reflection at 2θ = 6.4° was observed; it indicated an extended order in the chain–dopant–chain direction, wherein

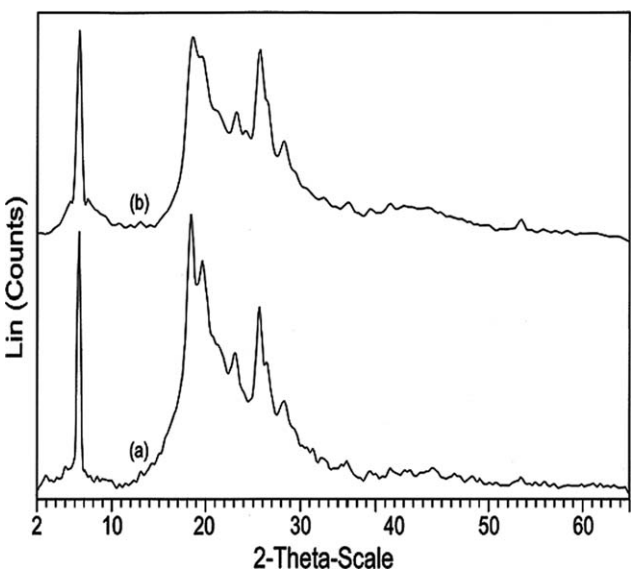

Figure 3 XRD patterns of PANI (a) base and (b) salt.

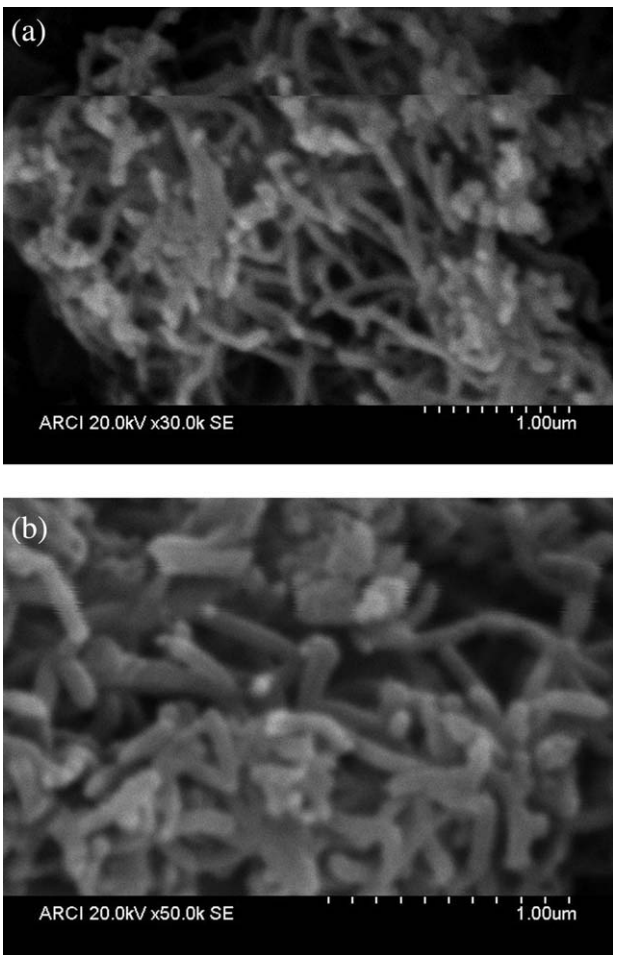

Figure 4 SEM pictures of the (a) PANI–H_2SO_4 salt and (b) PANI base.

the PANI chain distance increased by effective interdigitations of the dopant molecules. A similar pattern was reported for a PANI system with amphiphilic azobenzenesulfonic acid[34] and diesters of sulfosuccinic acid[35] dopants. Interestingly, the X-ray pattern of almost all of the PANI bases [Fig. 3(a)] prepared in this study were similar to that of the PANI salt.

SEM

The morphological characteristics of the PANI samples were examined by SEM. The PANI salt prepared at 60°C showed nanofibers with uniform diameter between 75 and 100 nm containing a netlike structure [Fig. 4(a)]. The morphology of the PANI nanofibers was not changed after dedoping with sodium hydroxide, but the fiber network slightly changed from a netlike structure to an agglomerate form, as shown in Figure 4(b). Huang and Kaner[36] reported PANI nanofiber synthesis at 100°C with the use of H_2SO_4 as a protic acid. In this study, PANI nanofibers were synthesized without any protic acid, and also, the PANI base showed nanofiber formation. The XRD spectrum of the PANI nanofibers showed a new peak formation at $2\theta = 6.5°$; this indicated the formation of a highly ordered PANI with a nanofiber morphology.

The IR, XRD, and SEM characterization of the PANI base confirmed that this polymer had characteristics similar to those of the PANI salt. The dedoping of the PANI salt by sodium hydroxide solution showed a reasonably good weight loss of sulfuric acid. These results indicate that the complete dedoping of PANI salt did not happen with the use of 1*M* aqueous sodium hydroxide solution. Interestingly, the characteristics of the PANI base, which contained very little of sulfuric acid dopant, showed a highly ordered structure with a nanofiber morphology.

ELECTROCHEMICAL STUDIES

The performances of PANI–H_2SO_4's as electrode materials for symmetric supercapacitors were investigated with CV, galvanostatic CD, and EIS measurements.

CV

CV was used to determine the electrochemical properties of a symmetric capacitor cell constructed with two PANI–H_2SO_4 salt electrodes in 1*M* H_2SO_4. CV was carried out in the voltage range −0.2 to 0.6 V at different scan rates (1, 5, and 10 mV/s; Fig. 5). Each curve was composed of a capacitive current, and the curves at different scan rates show no peaks; this indicated that the electrode was charged and discharged at a pseudo-constant rate over the complete voltammetric cycle. The capacitance (*C*) values for the symmetric capacitors were calculated from the

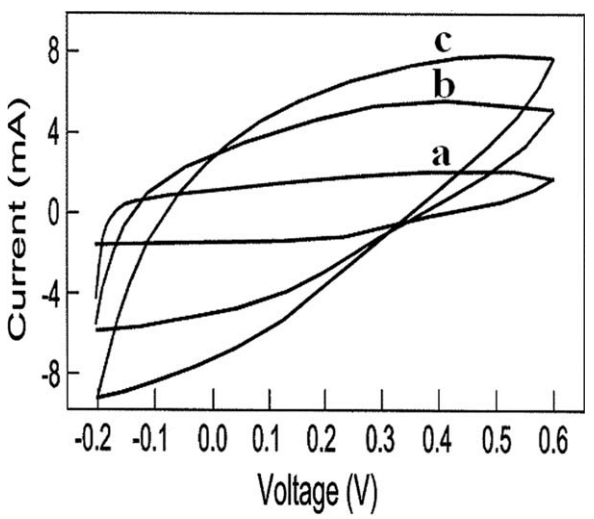

Figure 5 CV of the symmetric PANI–H_2SO_4 supercapacitor with 1*M* H_2SO_4 electrolyte at different sweep rates: (a) 1, (b) 5, and (c) 10 mV/s.

cyclic voltammograms with the following formula:

$$C = i/ms$$

where s is the potential sweep rate, m is the mass of the electrode, and i is the average current, and the results are reported in Table II. The capacitance value of PANI–H_2SO_4 increased with increasing the amount of APS, attained a maximum (182 F/g), and then decreased. A similar behavior was observed for the PANI–H_2SO_4 samples prepared at various times and temperatures. The maximum specific capacitance (273 F/g) was obtained with the use of 0.3*M* APS at 60°C for 6 h of reaction time.

Generally, the specific capacitance values decreased with increasing scan rates. As a representative system, the specific capacitance of PANI–H_2SO_4 prepared by 0.3*M* APS decreased to 182, 73, and 35 F/g at scan rates of 1, 5, and 10 mV/s, respectively. The decrease in capacitance with increasing scan rate may have been due to two reasons: (1) as the scan rate increased, it might have been difficult for the electric charge to occupy the available sites at electrode–electrolyte interface because of their limited range of migration and orientation in the electrolyte and (2) the internal resistance of the supercapacitor.[37]

CD studies

To better understand the behavior of the PANI–H_2SO_4 supercapacitor cell, galvanostatic charge–discharge values at various current densities of 1 and 5 mA were measured for PANI–H_2SO_4 salts, and the results are reported in Table II. The discharge specific capacitance (C_d), energy density (E), and power density (P) were calculated from the following formula:

$$C_d = I \times \Delta t/\Delta V \times m$$
$$E = \Delta V \times I \times \Delta t/3600 \times m$$
$$P = \Delta V \times I/m$$

where I is the charge–discharge current, Δt is the discharge time, ΔV is the voltage difference, and m is the mass of active material within the electrode. As a representative system, the values of the specific capacitance and energy and power densities for the PANI–H_2SO_4 system (prepared with 0.3*M* APS) discharged at 5 mA were found to be 43 F/g, 9.3 W h/Kg, and 500 W/Kg, respectively.

Generally, the specific capacitance calculated form CD was less than that found by CV measurements (Table II). As a representative system, the maximum specific capacitance obtained from CD (103 F/g) was less than that found by CV (273 F/g).

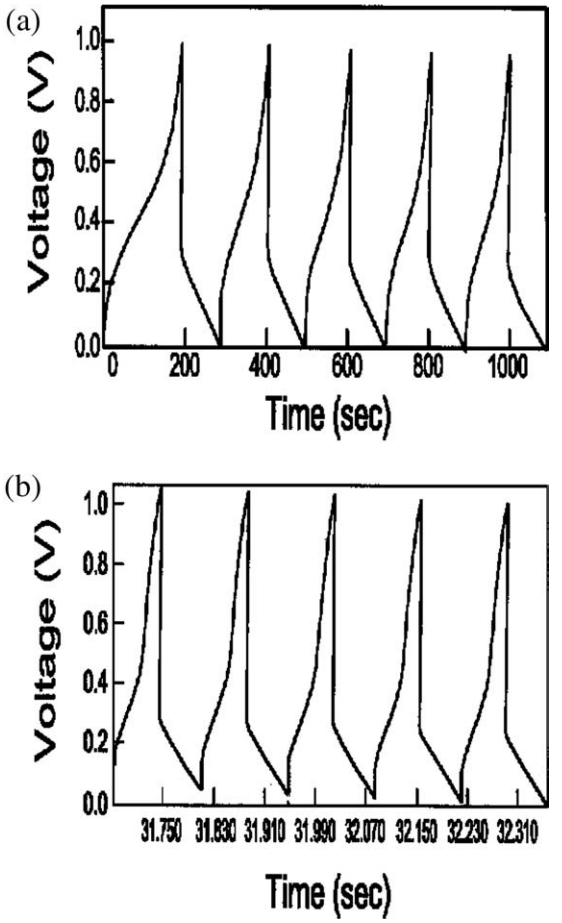

Figure 6 Galvanostatic charge and discharge of the PANI symmetric capacitor cell at a current density of 5 mA: (a) for the first five cycles and (b) for 196–200 cycles.

The galvanostatic CD behavior for the PANI–H_2SO_4 symmetric capacitor cell at a 5-mA current density between voltages of 0 and 1 V up to 200 cycles was also determined, and the performance data of the first five CD cycles [Fig. 6(a)] and the last five cycles [Fig. 6(b)] are reported. The nature of the curve remained almost the same, but the specific capacitance decreased from 43 F/g in the first cycle to 40 F/g after 100 cycles and then to 34 F/g after 200 cycles. This result indicates that the redox sites in the PANI backbone were insufficiently stable and underwent a slight degradation of the electrolyte and PANI electrodes during the repeated redox process. This was probably due to (1) expansion and contraction of PANI volume (this could be reduced with small-size dopants in the PANI salts or PANI–metal oxide composites) and (2) swelling and shrinking of PANI under an aqueous environment, which led to the degradation of PANI during long-term cycling.[38]

The reduction of capacitance with cycles has also been observed in the case of PANI–lithium salt from 100 to 70 F/g after 5000 cylces[39] and in the case of

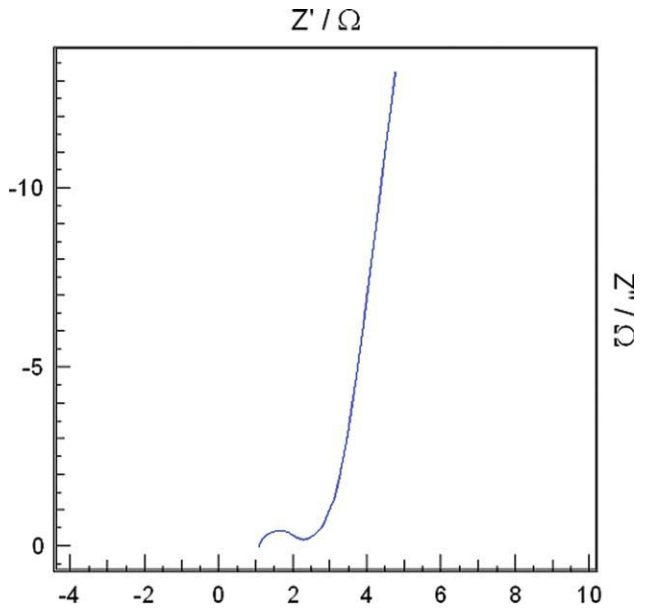

Figure 7 Impedance spectrum in the range 40 kHz–10 mHz of the PANI symmetric capacitor cell with a potential of 0.6 V. [z'- real impedance, z''- imaginary impedance]. [Color figure can be viewed in the online issue, which is available at wileyonlinelibrary.com.]

PANI–carbon system from 160 to 144 F/g over 1000 cycles.[38] The coulombic efficiencies (η's) of the capacitors were calculated with the following formula:

$$\eta = (t_D/t_C) \times 100$$

where t_D and t_C are expressions of the discharge and charge times, respectively. The columbic efficiency decreased slightly with the number of cycles from 100 to 98% at 200 cycles; this proved it to be a suitable material for supercapacitor applications.

Electrochemical impedance

The electrochemical behavior of PANI–H_2SO_4 was also examined by the EIS method. Impedance spectroscopy is a powerful tool for the mechanistic analysis of interfacial processes and for the evaluation of resistance, rate constants, capacitance, and so on. The Nyquist plot of PANI–H_2SO_4 salt prepared with 0.3*M* APS with a three-electrode cell configuration in 1.0*M* H_2SO_4 electrolyte is shown in Figure 7. The high-frequency region usually considered to reflect the bulk properties of the electrolyte and the medium-frequency region showed the impedance response of the charge transfer between the electrode and electrolyte. Also, the high-frequency region (semicircle portion) was attributed to a double-layer charging–discharging process. The frequency corresponding to the maximum (f^*) of the imaginary component ($-z''$) in the semicircle yielded the time constant (τ) as follows:

$$\tau = (1/2 \times \pi f^*)$$

The PANI–H_2SO_4 system showed τ values of 88.0, 84.1, and 7.1 ms with voltages of 0.6, 0.8, and 1.0 V, respectively, and this indicated fast CD characteristics. At low frequencies, the impedance is usually determined by the diffusion of ions into the polymer film; this gives a linear behavior with a frequency-independent phase angle of 45°. In the low-frequency region, the slope of the impedance plots increased and tended to become purely capacitive (a vertical line is characteristic of a limiting diffusion process). The capacitance was calculated from the following formula:

$$C = -(2\pi f z_{im})^{-1}$$

where, z_{im} represents imaginary impedance. The capacitance values for the PANI–H_2SO_4 system were calculated at a frequency of 0.01 Hz and were found to be 73.2, 72.7, and 65.7 F/g with voltages of 0.6, 0.8, and 1.0 V, respectively.

CONCLUSIONS

Highly ordered PANI–H_2SO_4 with a nanofiber morphology was synthesized by the simple oxidation of aniline by APS at a high temperature without any protic acid, wherein APS acted as an oxidizing agent and a protonating agent. PANI–H_2SO_4 showed netlike nanofibers with uniform diameter between 75 and 100 nm. Interestingly, PANI base was also obtained in a highly ordered structure with an agglomerated netlike nanofiber morphology. PANI salt was used as electrode material in a symmetric supercapacitor cell, and it showed a capacitance of 273 F/g with 98–100% coulombic efficiency.

This study was carried out at the Indian Institute of Chemical Technology, Hyderabad. The authors thank J. S. Yadav, Director, and B. S. Sitaramam, Head, Organic Coatings and Polymers Division, Indian Institute of Chemical Technology, Hyderabad, for the facilities and encouragement. Encouragement of this research study by the Council of Scientific and Industrial Research under the Solar Mission Project is gratefully acknowledged.

References

1. Obreja, V. V. N. Phys E 2008, 40, 2596.
2. Simon, P.; Gogotsi, Y. Nat Mater 2008, 7, 845.
3. Shukla, A. K.; Sampath, S.; Vijayamohanan, K. Curr Sci 2000, 79, 1656.
4. Cho, S.; Lee, S. B. Acc Chem Res 2008, 41, 699.
5. Jayalakshmi, M.; Balasubramanian, K. Int J Electrochem Sci 2008, 3, 1196.

6. Liu, J.; Cao, G.; Yang, Z.; Wang, D.; Dubois, D.; Zhou, X.; Graff, G. L.; Pederson, L. R.; Zhang, J. G. ChemSusChem 2008, 1, 676.
7. Li, L.; Liu, E.; Li, J.; Yang, Y.; Shen, H.; Huang, Z.; Xiang, X.; Li, W. J Power Sour 2010, 195, 1516.
8. Xinga, W.; Yuan, X.; Zhuo, S. P.; Huang, C. C. Polym Adv Technol 2009, 20, 1179.
9. Lixia, L.; Huaihe, S.; Qincang, Z.; Jingyuan, Y.; Xiaohong, C. J Power Sour 2009, 187, 268.
10. Amarnath, C. A.; Chang, J. H.; Kim, D.; Mane, R. S.; Han, S. H.; Sohn, D. Mater Chem Phys 2009, 113, 14.
11. Wang, H.; Hao, Q.; Yang, X.; Lu, L.; Wang, X. Electrochem Commun 2009, 11, 1158.
12. Mandić, Z.; Roković, M. K.; Pokupčić, T. Electrochim Acta 2009, 54, 2941.
13. Hu, Z. A.; Xie, Y. L.; Wang, Y. X.; Mo, L. P.; Yang, Y. Y.; Zhang, Z. Y. Mater Chem Phys 2009, 114, 990.
14. Bian, C.; Yu, A.; Wu, H. Electrochem Com 2009, 11, 266.
15. Mi, H.; Zhang, X.; Yang, S.; Ye, X.; Luo, J. Mat Chem Phys 2008, 112, 127.
16. Mi, H.; Zhang, X.; Ye, X.; Yang, S. J Power Sour 2008, 176, 403.
17. Sivakkumar, S. R.; Kima, W. J.; Choi, J. A.; MacFarlane, D. R.; Forsyth, M.; Kim, D. W. J Power Sour 2007, 171, 1062.
18. Song, R. K.; Park, J. H.; Sivakkumar, S. R.; Kim, S. H.; Ko, J. M.; Park, D. Y.; Jo, S. M.; Kim, D. Y. J Power Sour 2007, 166, 297.
19. Dong, B.; He, B. L.; Xu, C. L.; Li, H. L. Mater Sci Eng B 2007, 143, 7.
20. Mi, H.; Zhang, X.; An, S.; Ye, X.; Yang, S. Electrochem Com 2007, 9, 2859.
21. Yan, J.; Wei, T.; Fan, Z.; Qian, W.; Zhang, M.; Wei, F. J Power Sour 2010, 195, 3041.
22. Zheng, L.; Wang, Y.; Wang, X.; Li, N.; An, H.; Chen, H.; Guo, J. J Power Sour 2010, 195, 1747.
23. Subramania, A.; Devi, S. L. Polym Adv Technol 2008, 19, 725.
24. Koysuren, O.; Du, C.; Pan, N.; Bayram, G. J App Polym Sci 2009, 113, 1070.
25. Palaniappan, S.; Devi, S. L. J App Polym Sci 2008, 107, 1887.
26. Nikzad, L.; Alibeigi, S.; Vaezi, M. R.; Yazdani, B.; Reza, M.; Rahimipour, M. R. Chem Eng Technol 2009, 32, 861.
27. Appel, G.; Yfantis, A.; Gopel, W.; Schmeiber, D. Synth Met 1996, 83, 197.
28. Albuquerque, J. E.; Mattoso, L. H. C.; Faria, R. M.; Masters, J. G.; MacDiarmid, A. G. Synth Met 2004, 146, 1.
29. Mattoso, L. H. C.; MacDiarmid, A. G. Polymeric Materials Encyclopedia; CRC: New York, 1996; Vol.7, p 5505.
30. Kang, T.; Neoh, K. G.; Tan, K. L. Prog Polym Sci 1998, 23, 277.
31. Furukawa, Y.; Ueda, F.; Hyodo, Y.; Harada, I.; Nakajima, T.; Kawagoe, T. Macromolecules 1988, 21, 1297.
32. Wusheng Yin, W.; Ruckenstein, E. Macromolecules 2000, 33, 1129.
33. Pouget, J. P.; Jozefowicz, M. E.; Epstein, A. J.; Tang, X.; MacDiarmid, A. G. Macromolecules 1991, 24, 779.
34. Anilkumar, P.; Jayakannan, M. Macromolecules 2007, 40, 7311.
35. Dufour, B.; Rannou, P.; Djurado, D.; Janeczek, H.; Zagorska, M.; Geyer, A.; Travers, J. P.; Pron, A. Chem Mater 2003, 15, 1587.
36. Huang, J.; Kaner, R. B. Chem Commun 2006, 4, 367.
37. Sivaraman, P.; Rath, S. K.; Hande, V. R.; Thakur, A. P.; Patri, M.; Samui, A. M. Synth Met 2006, 156, 1057.
38. Chen, W. C.; Wen, T. C. J Power Sources 2003, 117, 273.
39. Ryu, K. S.; Kim, K. M.; Park, Y. J.; Park, N. G.; Kang, M. G.; Chang, S. H. Solid State Ionics 2002, 152–153, 861.